EPR Spectrum of $Mn(\eta\text{-}C_4H_6)_2PMe_3$ in Single Crystals of Its Iron Analogue: Orientation of g and Hyperfine Tensors in the Unit Cell[1]

J. M. McCall, J. R. Morton, Y. Le Page, and K. F. Preston*

Division of Chemistry, National Research Council of Canada, Ottawa, Ontario, Canada K1A 0R9

Received February 3, 1984

The crystal structure of $Fe(\eta\text{-}C_4H_6)_2PMe_3$ has been determined; it crystallizes in the monoclinic system with space group $P2_1/c$. Unit cell dimensions are a = 7.729 (2) Å, b = 21.204 (4) Å, and c = 8.096 (2) Å with β = 115.18 (2)°. The unit cell contains four molecules and has a calculated density of 1.328 g cm^{-3}. In addition the EPR spectra of $Fe(\eta\text{-}C_4H_6)_2PMe_3$ doped with ca. 0.4% $Mn(\eta\text{-}C_4H_6)_2PMe_3$ were examined at 100 K. The spectra indicate that the unpaired electron occupies an orbital that is predominantly Mn $3d_{z^2}$ directed along the Mn–P bond.

Introduction

A recent claim[2] that the electronic structure of manganese-centered radicals of the type $Mn(\eta\text{-}C_4H_6)_2L$ differed substantially from that of the prototype $Mn(CO)_5$[3,4] prompted us to examine the EPR spectra of such species in single-crystal hosts. Our experiments[5] with $Mn(\eta\text{-}C_4H_6)_2PMe_3$ doped into single crystals of the diamagnetic iron analogue showed that differences from $Mn(CO)_5$ were, in fact, more apparent than real and arose from difficulties inherent in the interpretation of powder EPR spectra. Unfortunately, the crystal structure of $Fe(\eta\text{-}C_4H_6)_2PMe_3$ was not established at the time of our EPR experiments, so that we were not able to determine the principal directions of the **g** and hyperfine tensors in the host lattice. This situation has now been rectified, and we are able to correlate our EPR data with the crystal structure of $Fe(\eta\text{-}C_4H_6)_2PMe_3$. The results substantiate our earlier conclusion[5] that in $Mn(\eta\text{-}C_4H_6)_2PMe_3$ the dominant Mn atomic orbital component of the semioccupied molecular orbital (SOMO) is $3d_{z^2}$ directed along the Mn–P bond.

Experimental Section

The compounds $Fe(\eta\text{-}C_4H_6)_2PMe_3$ and $Mn(\eta\text{-}C_4H_6)_2PMe_3$ were prepared and purified according to published procedures.[2,5] Single crystals of the iron compound, both pure and doped with ca. 0.4% manganese analogue, were grown by sublimation.

X-ray diffraction intensity measurements were carried out at 300 K with graphite-monochromatized Mo Kα radiation on a crystal of approximate dimensions 0.2 × 0.2 × 0.3 mm mounted on a four-circle diffractometer. Mn-doped crystals mounted on Pyrex fibers were prealigned on the diffractometer and subsequently glued in a known orientation to the gear wheel of a two-circle EPR goniometer[6] with epoxy cement. Single-crystal EPR studies[7] with this goniometer were performed at 100 K in the cavity of a Varian E12 spectrometer, using standard accessories for field intensity and microwave frequency measurements. It is estimated that crystal transfer between the goniometers resulted in a misorientation of no more than 5°.

Results

(a) Crystallography. It was found that $Fe(\eta\text{-}C_4H_6)_2PMe_3$ crystallizes in the monoclinic system with space group $P2_1/c$. Unit cell dimensions refined from the Bragg angles of 10 reflections were a = 7.729 (2) Å, b = 21.204 (4) Å, c = 8.096 (2) Å, and β = 115.18 (2)°. The unit cell contains four molecules and has a calculated density of 1.328 g cm^{-3}.

Of a total of 1585 measured reflection intensities, data for 981 reflections with $I > 3\sigma(I)$ were retained and used in the structure analysis. Least-squares refinement of all positional and thermal parameters by the block-diagonal method converged at R_1 = 0.029 and R_2 = 0.018. Atomic coordinates are given in Table I.

(b) EPR Data. Insofar as the EPR spectrum is concerned, the system $Mn(\eta\text{-}C_4H_6)_2PMe_3$ in single crystals of $Fe(\eta\text{-}C_4H_6)_2PMe_3$ is a one-site system, a fact which led us to suggest earlier[5] that crystals of $Fe(\eta\text{-}C_4H_6)_2PMe_3$ were triclinic. Since the crystals are in fact monoclinic, two of the three principal directions of the **g** and hyperfine tensors must lie in the ac plane, the third principal direction lying along b.[7,9] Accordingly, a crystal was mounted on the two-circle goniometer so that the magnetic field could explore the ac plane. The results are shown in Figure 1, in which (a) the ^{55}Mn hyperfine interaction and (b) the $\mathbf{g}^2$ variation are plotted against angle from $+a^*$ in the ac plane, and a sinusoidal function fitted to them.[7] Note that the two tensors are coaxial; i.e., maximum hyperfine interaction and minimum g are coincident (within experimental error) at 32° from a^*. Two of the three principal values of the ^{55}Mn hyperfine and $\mathbf{g}^2$ tensors can be obtained from the turning points of the best-fit curves in Figure 1; the third principal value of each tensor was obtained by manipulating the goniometer to place H_0 along b.

A summary of the EPR data in tensor form for $Mn(\eta\text{-}C_4H_6)_2PMe_3$ in a single crystal of $Fe(\eta\text{-}C_4H_6)_2PMe_3$ is given in Table II, on the right-hand side of which are shown the principal values of the various tensors and their direction cosines referred to the a^*bc axis system. Since all three tensors are coaxial, it is not necessary to obtain the tensor $\mathbf{g}^{-1}$ in order to compute $\mathbf{a}^2 = \mathbf{g}^{-1}(\mathbf{g}\mathbf{a}^2\mathbf{g})\,\mathbf{g}^{-1}$, the hyperfine interaction squared in MHz^2. One can simply divide the principal values of the $\mathbf{g}^2\mathbf{a}^2$ tensor in Table II by the ap-

(1) NRCC No. 23340.
(2) Harlow, R. L.; Krusic, P. J.; McKinney, R. J.; Wreford, S. S. *Organometallics* **1982**, *1*, 1506.
(3) Howard, J. A.; Morton, J. R.; Preston, K. F. *Chem. Phys. Lett.* **1981**, *83*, 226.
(4) Symons, M. C. R.; Sweany, R. L. *Organometallics* **1982**, *1*, 834.
(5) McCall, J. M.; Morton, J. R.; Preston, K. F. *Organometallics*, **1984**, *3*, 238.
(6) Morton, J. R.; Preston, K. F.; Strach, S. J. *Rev. Sci. Instrum.* **1981**, *52*, 1358.
(7) Morton, J. R.; Preston, K. F. *J. Magn. Reson.* **1983**, *52*, 457.
(8) Huttner, G.; Neugebauer, D.; Razavi, A. *Angew. Chem., Int. Ed. Engl.* **1975**, *14*, 352.
(9) Weil, J. A.; Buch, T.; Clapp, J. E. *Adv. Magn. Reson.* **1973**, *6*, 183.

0276-7333/84/2303-1299$01.50/0 Published 1984 by the American Chemical Society

Table I. Atomic Parameters x, y, and z and B_{eq}[a]

	x	y	z	B_{eq} or B, Å^2
Fe	0.28405 (8)	0.87915 (3)	0.13951 (7)	2.76 (3)
P	0.56329 (14)	0.87543 (6)	0.37816 (13)	3.20 (6)
C1	0.2493 (6)	0.78454 (19)	0.1866 (5)	4.7 (3)
C2	0.0773 (6)	0.81302 (20)	0.0695 (5)	5.0 (3)
C3	0.0191 (5)	0.86823 (21)	0.1270 (5)	4.7 (3)
C4	0.1354 (5)	0.89107 (20)	0.2998 (5)	4.7 (3)
C5	0.4395 (6)	0.86920 (20)	−0.0163 (5)	4.4 (3)
C6	0.2538 (6)	0.89017 (20)	−0.1200 (5)	4.9 (3)
C7	0.1912 (6)	0.94381 (20)	−0.0628 (5)	4.7 (3)
C8	0.3124 (6)	0.97494 (18)	0.0958 (5)	4.5 (3)
CM1	0.5687 (6)	0.86704 (24)	0.6048 (5)	5.9 (3)
CM2	0.7210 (6)	0.81029 (20)	0.3875 (6)	5.4 (3)
CM3	0.7247 (6)	0.94168 (21)	0.4227 (5)	5.1 (3)
H1A	0.289 (4)	0.7500 (14)	0.139 (4)	5.2 (9)
H1B	0.283 (4)	0.7781 (12)	0.309 (3)	2.7 (7)
H2	0.018 (5)	0.7975 (16)	−0.052 (4)	7.0 (10)
H3	−0.101 (4)	0.8933 (16)	0.023 (4)	6.7 (10)
H4A	0.117 (4)	0.9322 (13)	0.322 (4)	3.7 (8)
H4B	0.204 (4)	0.8642 (13)	0.420 (4)	4.1 (8)
H5A	0.467 (4)	0.8252 (14)	−0.036 (4)	4.9 (9)
H5B	0.545 (4)	0.8941 (13)	0.025 (4)	3.3 (8)
H6	0.158 (4)	0.8627 (13)	−0.213 (3)	4.4 (8)
H7	0.051 (4)	0.9540 (15)	−0.126 (4)	5.5 (9)
H8A	0.267 (5)	1.0104 (16)	0.159 (5)	8.8 (12)
H8B	0.428 (3)	0.9816 (11)	0.112 (3)	1.2 (6)
HM1A	0.711 (5)	0.8688 (17)	0.707 (4)	8.5 (11)
HM1B	0.511 (5)	0.8247 (18)	0.610 (5)	9.6 (13)
HM1C	0.505 (5)	0.8992 (16)	0.616 (4)	8.1 (12)
HM2A	0.829 (5)	0.8098 (18)	0.501 (5)	8.7 (12)
HM2B	0.733 (4)	0.8098 (13)	0.281 (4)	4.1 (8)
HM2C	0.648 (5)	0.7664 (18)	0.357 (5)	10.6 (14)
HM3A	0.839 (4)	0.9339 (17)	0.532 (5)	7.9 (11)
HM3B	0.655 (4)	0.9807 (16)	0.445 (5)	7.5 (11)
HM3C	0.745 (4)	0.9517 (14)	0.318 (4)	5.6 (9)

[a] Esds refer to the last digit printed. B_{eq} is the arithmetic mean of the principal axes of the thermal ellipsoid for non-H atoms. H atoms were refined isotropically.

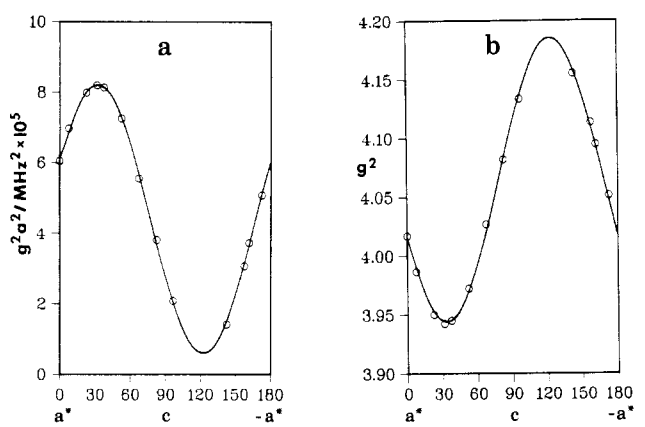

Figure 1. Graphs of (a) ^{55}Mn hyperfine interaction and (b) g^2 for $Mn(\eta\text{-}C_4H_6)_2PMe_3$ trapped in a single crystal of $Fe(\eta\text{-}C_4H_6)_2PMe_3$. Data points are circles; the line is a least-squares sinusoidal fit to them.

propriate principal values of $\mathbf{g}^2$. A further division of a/MHz by $g\beta$ gives the principal values in the customary units of gauss.

xx: g = 2.0301, a_{Mn} = 57.4, a_P = 25

yy: g = 2.0458, a_{Mn} = 41.7, a_P = 26

zz: g = 1.9860, a_{Mn} = 164.0, a_P = 28

Here, x is coincident with b, while z is 32° from a^* in the $+a^*$, $+c$ quadrant.

Discussion

(a) Crystal Structure of $Fe(\eta\text{-}C_4H_6)_2PMe_3$. A perspective drawing of the molecule showing the atom numbering scheme is shown in Figure 2. A stereoview and a [010] projection of the unit cell are shown in Figures 3 and 4, respectively. Selected bond lengths and angles are given in Table III.

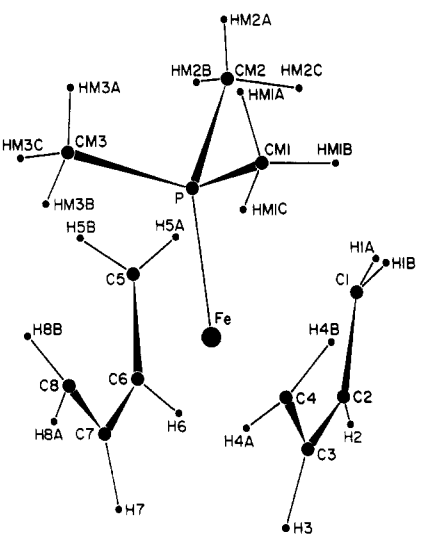

Figure 2. Structure of the molecule $Fe(\eta\text{-}C_4H_6)_2PMe_3$ (interatomic parameters are in Table III).

The molecular structure of $Fe(\eta\text{-}C_4H_6)_2PMe_3$ consists of an iron atom square pyramidally coordinated by one apical PMe_3 and two basal *cis*-butadiene ligands. Although not crystallographically imposed, there is an approximate mirror plane connecting the two butadienes and containing the Fe–P vector. Free 1,3-butadiene has a terminal C=C bond length of 1.36 Å and a central C—C bond length of 1.45 Å.[10] Coordination to an iron center results in a

Table II. Tensors of g^2 and g^2a^2/MHz^2 [a] (^{55}Mn and ^{31}P) in the a^*bc Axis System for $Mn(\eta\text{-}C_4H_6)_2PMe_3$ in a Single Crystal of $Fe(\eta\text{-}C_4H_6)_2PMe_3$

	tensor in a^*bc axes			principal values and their direction cosines	
	a^*	b	c		
g^2	4.0165	0	−0.1104	x	4.1213 (0, 1, 0)
	0	4.1213	0	y	4.1854 (−0.5470, 0, 0.8371)
	−0.1104	0	4.1133	z	3.9444 (0.8371, 0, 0.5470)
^{55}Mn	6.0513	0	3.4253	x	1.0962 (0, 1, 0)
	0	1.0962	0	y	0.5962 (−0.5318, 0, 0.8469)
	3.4253	0	2.7470	z	8.2021 (0.8469, 0, 0.5318)
^{31}P	0.2368	0	0.0032	x	0.208 (0, 1, 0)
	0	0.208	0	y	0.232 (−0.5529, 0, 0.8333)
	0.0032	0	0.2341	z	0.239 (0.8333, 0, 0.5529)

[a] Units of g^2a^2 are $(MHz)^2 \times 10^5$.

Table III. Selected Bond Distances and Angles for $Fe(\eta\text{-}C_4H_6)_2PMe_3$

Bond Distances (Å)

Fe-P	2.202 (1)	Fe-C3	2.020 (4)	Fe-C6	2.026 (4)
Fe-C1	2.080 (4)	Fe-C4	2.083 (4)	Fe-C7	2.019 (4)
Fe-C2	2.017 (4)	Fe-C5	2.090 (4)	Fe-C8	2.089 (4)
P-CM1	1.826 (4)	P-CM2	1.822 (4)	P-CM3	1.810 (4)
C1-C2	1.399 (6)	C2-C3	1.403 (6)	C3-C4	1.390 (6)
C5-C6	1.392 (6)	C6-C7	1.391 (6)	C7-C8	1.393 (6)

Bond Angles (deg)

Fe-P-CM1	118.7 (1)	Fe-P-CM2	116.9 (1)	Fe-P-CM3	118.8 (1)
P-Fe-C1	87.7 (1)	P-Fe-C2	125.8 (1)	P-Fe-C3	129.4 (1)
P-Fe-C4	93.0 (1)	P-Fe-C5	85.7 (1)	P-Fe-C6	123.5 (1)
P-Fe-C7	127.8 (1)	P-Fe-C8	92.8 (1)	CM1-P-CM2	98.9 (2)
CM1-P-CM3	99.0 (2)	CM2-P-CM3	100.8 (2)	C1-Fe-C4	81.6 (2)
C1-Fe-C8	178.1 (2)	C1-Fe-C5	99.5 (2)	C4-Fe-C5	178.2 (2)
C1-C2-C3	118.8 (4)	C4-C3-C2	117.6 (4)	C5-C6-C7	118.4 (4)
C8-C7-C6	120.1 (4)				

Distances (Å) from Least-Squares Planes[a]

plane defined by $C_1C_2C_3C_4$		plane defined by $C_5C_6C_7C_8$	
atom	dist, Å	atom	dist, Å
H1A	0.08	H5A	0.28
H1B	−0.54	H5B	−0.56
H2	0.13	H6	0.23
H3	0.18	H7	0.16
H4A	0.26	H8A	0.17
H4B	−0.58	H8B	−0.53

[a] Distances ±0.04 Å. Sign convention: +, toward Fe: −, away from Fe.

shortening of the central C—C bond length relative to the terminal C=C bonds as the double bonds become less localized. In $Fe(\eta\text{-}C_4H_6)(CO)_3$ the central and terminal bonds are experimentally equal at 1.45 (6) and 1.46 (5) Å, respectively.[11] In $Fe(\eta\text{-}C_4H_6)_2CO$ the central and terminal bond lengths are 1.46 (1) and 1.43 (2) Å, respectively.[12] In the isomorphous manganese complex $Mn(\eta\text{-}C_4H_6)_2CO$, the central and terminal C–C bonds are more distinct with lengths of 1.46 (1) and 1.39 (1) Å, respectively.[8] Replacement of the CO ligand in $Fe(\eta\text{-}C_4H_6)_2CO$ with a PMe_3 ligand to give the host complex of this study gave rise to small changes in the butadiene bond lengths. The four terminal C–C bonds shorten to 1.394 (6) Å (average) and the two central C–C bonds shorten to 1.397 (6) Å (average) so that all C–C bond lengths are equal within experimental error.

The shorter (by ca. 0.07 Å) Fe–C(central) and Fe–C(terminal) bond distances in $Fe(\eta\text{-}C_4H_6)_2PMe_3$ compared with those in $Fe(\eta\text{-}C_4H_6)_2CO$ are consistent with a strengthening of the Fe–C(butadiene) bonds. The central and terminal L–Fe–C angles are independent of axial ligand (L = CO, PMe_3) within experimental error (Table IV).

Table IV. Certain Averaged Bond Lengths (Å) and Angles (deg) in $Fe(\eta\text{-}C_4H_6)_2L$

	L = CO	L = PMe_3
Fe-C(central)	2.09 (1)	2.021 (4)[a]
Fe-C(terminal)	2.16 (1)	2.086 (4)[a]
L-Fe-C(central)	126.3 (5)	126.6 (1)[a]
L-Fe-C(terminal)	89.3 (5)	89.8 (1)[a]

[a] Average of four values.

Table V. Partial ^1H NMR Spectra for $Fe(\eta\text{-}C_4H_6)_2L$[a]

L			
CO[b]	$P(OMe)_3$[c]	PMe_3[d]	assignmt
−0.37	−0.70	−1.22	anti CH*H*
1.03	1.00	0.92	syn CH*H*
4.32	4.41	4.33	CH

[a] Solvent benzene-d_6 unless stated otherwise; chemical shifts in δ (ppm). [b] Reference 16. [c] Ittel, S. D.; Van-Catledge, F. A.; Jesson, J. P. *J. Am. Chem. Soc.* 1979, *101*, 3874. Solvent not reported. [d] Reference 5.

(10) Cotton, F. A.; Wilkinson, G. "Advanced Inorganic Chemistry", 3rd ed.; Wiley-Interscience: New York, 1972; p 732.
(11) Mills, O. S.; Robinson, G. *Acta Crystallogr.* **1963**, *16*, 758.
(12) Whiting, D. A. *Cryst. Struct. Commun.* **1972**, *1*, 379.

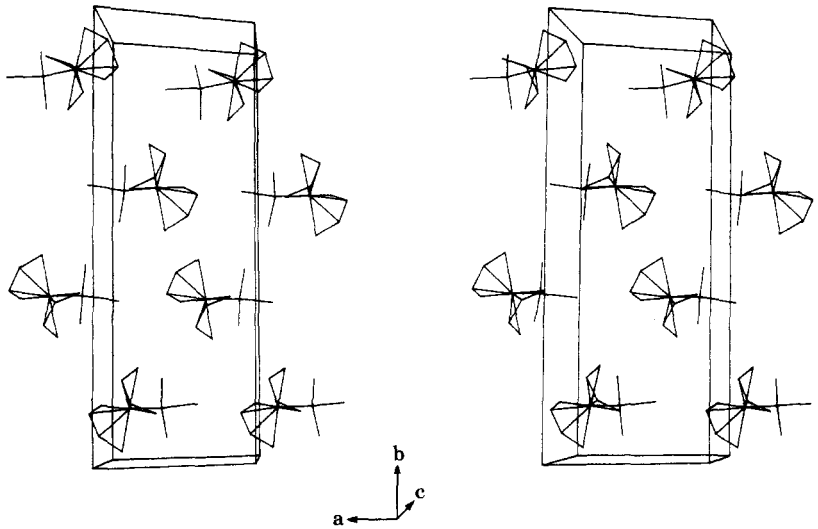

Figure 3. Stereogram of unit cell of $Fe(\eta\text{-}C_4H_6)_2PMe_3$.

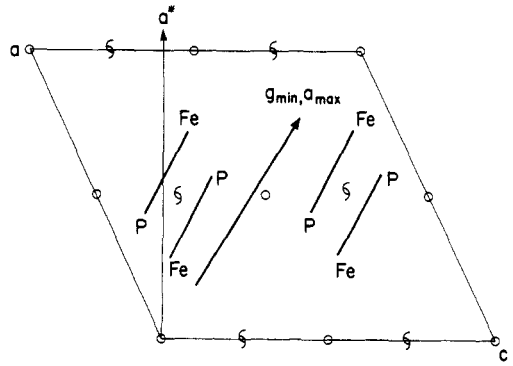

Figure 4. Projection of the Fe–P bonds of $Fe(\eta\text{-}C_4H_6)_2PMe_3$ on to the *ac* plane.

Thus the greater steric requirement of the PMe_3 ligand compared with the CO group (cone angles[13] 118° and ca. 95°, respectively) is not evident in $Fe(\eta\text{-}C_4H_6)_2PMe_3$.

Trialkylphosphine ligands are strong σ donors that increase electron density at a metal center,[14] but they are poorer π acceptors than CO.[15] Trialkyl phosphites are intermediate in effect. This distinction in electronic effects is evident from the partial ^1H NMR spectra of three complexes of the type $Fe(\eta\text{-}C_4H_6)_2L$, where L = CO, $P(OMe)_3$, and PMe_3 (Table V). On the basis of the the signal assignments by Carbonero and Greco[16] for $Fe(\eta\text{-}C_4H_6)_2CO$ the ^1H NMR spectrum[5] of **1** has been assigned analogously. The multiplet at $\delta \sim 4$ is assigned to the central protons, the broad doublet at $\delta \sim 1$ to the syn CH_2 protons, and the multiplet at highest field to the anti CH_2 protons. As the σ-donor strength increases in the order CO < $P(OMe)_3$ < PMe_3, the signals for the syn and anti CH_2 protons are found at increasingly higher field. The central protons of the butadiene ligand do not seem to be affected greatly by the ligand L.

The hydrogen atoms of the butadiene ligands were resolved in our crystal analysis of $Fe(\eta\text{-}C_4H_6)_2PMe_3$. None of these atoms lay in the least-squares plane containing the carbon atoms of each butadiene group. The syn hydrogens of the terminal CH_2 groups (H1A, H4A, H5A, and H8A in Figure 2) lie between 0.08 and 0.28 Å from the planes toward the Fe atom, while the anti hydrogens (H1B, H4B, H5B, and H8B) lie between 0.53 and 0.58 Å from the planes away from the metal atom. The central H atoms lie from 0.13 to 0.23 Å toward the Fe atom (Table III). These locations are similar to those reported for (butadiene)(cyclooctatetraene)iron carbonyl, $Fe(\eta\text{-}C_4H_6)(\eta^4\text{-}C_8H_8)CO$, where the anti hydrogens were 0.56 Å above the butadiene plane away from the iron center while the syn hydrogens were 0.21 Å below the plane toward iron.[17] As in $Fe(\eta\text{-}C_4H_6)_2PMe_3$, the central hydrogens of the butadiene ligand were 0.10 Å below the plane toward iron.[17] Similarly, the X-ray structure of $Mn(\eta\text{-}C_4H_6)_2P(OMe)_3$ showed methine and syn hydrogens out of the butadiene planes directed toward the metal and anti hydrogens directed away from the manganese.[2]

Table VI. Angles (deg) between Tensor Principal Axes and Selected Interatomic Vectors

	xx	*yy*	*zz*
PFe	92	95	5
C1Fe	165	75	88
C8Fe	14	104	92
C4Fe	83	8	87
C5Fe	96	174	91

(b) Tensor Orientations. The lack of site splitting noted for the EPR spectrum of $Mn(\eta\text{-}C_4H_6)_2PMe_3$ in the monoclinic crystal of $Fe(\eta\text{-}C_4H_6)_2PMe_3$ demonstrates that the magnetic tensors have one principal axis parallel to the crystal *b* axis and two principal axes in *ac*.[7,9] The crystallographic data show that all Fe–P bonds of the host structure lie within 2° of the *ac* plane and that their projections in that plane (Figure 4) are parallel and lie 27° from *a** in the first *a***c* quadrant. This direction coincides, within the error of transfer between goniometers, with the direction of minimum **g** and maximum ^{55}Mn hyperfine components. Assuming that the manganese analogue impurity adopts the orientation of the host molecules, we deduce that the Mn atomic orbital contribution to the SOMO of $Mn(\eta\text{-}C_4H_6)_2PMe_3$ is $3d_{z^2}$ directed along, or nearly along, the metal–phosphorus bond. This inference reinforces our earlier conclusion[5] that the radical has a structure analogous to that of $Mn(CO)_5$.

The low symmetry (C_s) of the paramagnetic site permits admixture[18] of a small amount of $d_{x^2-y^2}$ character into the SOMO. We have previously estimated[5] that such a con-

(13) Tolman, C. A. *Chem. Rev.* **1977**, *77*, 313.
(14) Parshall, G. W. "Homogeneous Catalysis"; Wiley-Interscience: New York, 1980; p 11.
(15) Cotton, F. A.; Wilkinson, G. "Advanced Inorganic Chemistry", 3rd ed.; Wiley-Interscience: New York, 1972; p 720.
(16) Carbonero, A.; Greco, A. *J. Organomet. Chem.* **1970**, *25*, 477.
(17) Bassi, I. W.; Scordamaglia, R. *J. Organomet. Chem.* **1972**, *37*, 353.
(18) McGarvey, B. R. *Can. J. Chem.* **1975**, *53*, 2498.

tribution of $d_{x^2-y^2}$ to the SOMO is less than 1% of that from d_{z^2}.

Of the remaining principal axes, one of them (x) necessarily lies along the crystal b axis, and the other (y) is then forced to lie in ac perpendicular to the Fe–P bond. The fact (see Table VI) that these directions nearly coincide with certain Fe–C vectors is purely accidental. Crystal forces evidently dictate the orientation of the x and y tensor components in this case.

Some site splitting may, of course, be hidden in the linewidth (~20 G). This is a likely possibility in a system where one principal axis and turning point is close to a crystal symmetry axis. In other words, Mn($3d_{z^2}$) may lie precisely along the Fe–P vector of the crystal with x directed 2° from b, yet site splitting would not be detected.

Registry No. Fe(η-C_4H_6)$_2$PMe$_3$, 87922-45-0; Mn(η-C_4H_6)$_2$PMe$_3$, 82963-75-5.

Supplementary Material Available: Tables of anisotropic temperature factors and observed and calculated structure factors for Fe(η-C_4H_6)$_2$PMe$_3$ (9 pages). Ordering information is provided on any current masthead page.

Electrochemistry of Phosphaferrocenes. 1. Comparison of the Redox Properties of Ferrocene, Diphosphaferrocene, 3,4-Dimethyl-1-phosphaferrocene, and 3,3′,4,4′-Tetramethyl-1,1′-diphosphaferrocene

Paul Lemoine,*[1a] Maurice Gross,[1a] Pierre Braunstein,[1b] François Mathey,[1c] Bernard Deschamps,[1c] and John H. Nelson[1d]

Laboratoire d'Electrochimie et de Chimie Physique du Corps Solide, ERA au CNRS No. 468, Université Louis Pasteur, 67000, Strasbourg, France, Laboratoire de Chimie de Coordination, ERA au CNRS No. 670, Université Louis Pasteur, 67000 Strasbourg, France, Equipe CNRS/SNPE, 94320 Thiais, France, and the Department of Chemistry, University of Nevada, Reno, Nevada, 89557

Received November 28, 1983

The redox behavior of three phosphaferrocenes (hereafter referred to as **1**, **2**, and **3**) has been investigated

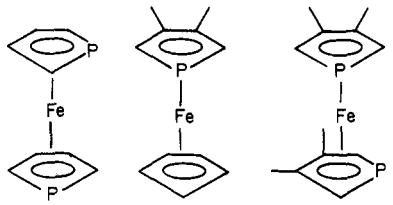

on both solid (Pt, Au, vitreous carbon) and dropping mercury electrodes in solvents with varying donicities and compared with the redox behavior of ferrocene (Fc). It was found that the replacement of a CH group by a phosphorus atom strongly modifies the reduction potential. Reversible one-electron reductions in propylene carbonate occur at $E_{1/2}$ = −2.15 V vs. SCE for **1**, at −2.33 V for **3**, and at −2.55 V for **2** compared to −2.93 V for Fc. The phosphaferrocenes also undergo one-electron oxidations at potentials near that for the oxidation of Fc (Fc (+0.40 V), **1** (+0.78 V), **3** (+0.57 V), **2** (+0.52 V)). The stability of the derived phosphaferricinium cations depends upon the solvent nature. In general, the phosphaferricinium cations are less stable than the ferricinium cation, but the ESR spectrum of the $3^{+\cdot}$ cation has been obtained and it displays no hyperfine coupling. The unpaired electron is localized largely on iron. The redox potentials display additivity and can be predicted by assigning group contributions to the P and CH_3 groups. Complexes **2** and **3** also exhibit an irreversible two-electron oxidation that is attributed to oxidation on ligands of 2^+ and 3^+ by comparison with the oxidation of an analogous phosphole. The experimental results are discussed in terms of the HOMO and LUMO levels as determined by recent quantum mechanical calculations. The heterogeneous rate constants of the electron transfer are calculated.

Introduction

In the recent years, the Fc/Fc$^+$ couple and derivatives[2-24] = ferrocene, (η^5-C_5H_5)$_2$Fe) attracted much interest owing to the ability of Fc/Fc$^+$ to function as a reference system in nonaqueous media in the general context of the steep

(1) (a) Laboratoire d'Electrochimie. (b) Laboratoire de Chimie de Coordination. (c) CNRS/SNPE. (d) University of Nevada.
(2) Page, J. A.; Wilkinson, G. *J. Am. Chem. Soc.* **1952**, *74*, 6149.
(3) Reinolds, L. T.; Wilkinson, G. *J. Inorg. Nucl. Chem.* **1959**, *9*, 86.
(4) Headridge, J. B.; Ashraf, M.; Dodds, N. L. H. *J. Electroanal. Chem. Interfacial Electrochem.* **1968**, *16*, 114.
(5) Bublitz, D. E.; Hoh, G.; Kuwana, T. *Chem. Ind. (London)* **1959**, 635.
(6) El Murr, N.; Chaloyard, A.; Laviron, E. *Nouv. J. Chim.* **1978**, *2*, 15.
(7) Tirouflet, J.; Boichard, J. *C.R. Hebd. Seances Acad. Sci.* **1960**, 1861.
(8) Tirouflet, J.; Dabard, R.; Laviron, E. *Bull. Soc. Chim. Fr.* **1963**, 1655.

0276-7333/84/2303-1303$01.50/0